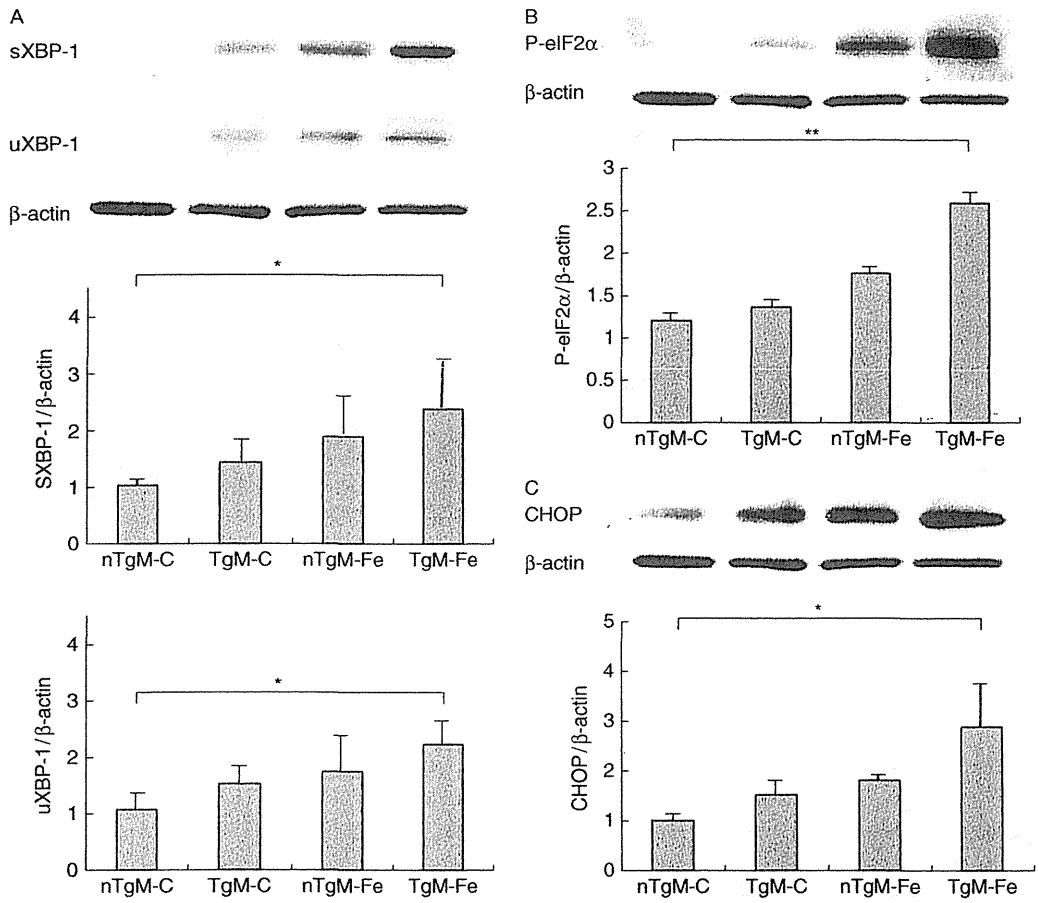

Fig. 3. Expression of spliced X-box DNA-binding protein 1 (sXBP-1), unspliced X-box DNA-binding protein 1 (uXBP-1), phosphorylated eukaryotic initiation factor-2α (p-eIF2α) and CCAAT/enhancer-binding protein homology protein (CHOP) in the liver. Immunoblots for sXBP-1 and uXBP-1 (A), p-eIF2α (B) and CHOP (C) were performed using liver lysates obtained from seven full-length HCV-N open reading frame (FL-N/35) transgenic mice fed the excess-iron diet and four mice in the three other groups at 12 months after initiation of iron loading. The protein expression was normalized with β-actin. $^{*}P < 0.05$, $^{**}P < 0.01$. nTgM-C, TgM-C, nTgM-Fe, and TgM-Fe; see legend for Figure 1.

and was assessed with the sXBP-1 protein level (22). PERK activation was evaluated by measurement of p-eIF2α and CHOP (23). ATF6 activation was assessed with uXBP-1 expression (24). The expression of uXBP-1, sXBP1, p-eIF2α and CHOP was significantly greater in FL-N/35 transgenic mice fed the excess-iron diet than that in nontransgenic mice fed the control diet (Fig. 3).

Autophagy

We next examined the formation of autophagosomes at the ultrastructural level to confirm the activation of the unfolded protein response, because autophagy has been shown to be induced by the unfolded protein response (25–27). As shown in Figure 4, autophagosomes (indicated by arrows) were abundantly found in the liver in FL-N/35 transgenic mice fed the excess-iron diet. In contrast, autophagosomes were not present in the liver of nontransgenic mice fed the excess-iron diet. These results were compatible with the increased expression of uXBP1, sXBP1, p-eIF-2α and CHOP in FL-N/35 transgenic mice fed the excess-iron diet, suggesting activation of the unfolded protein response. Thus, activation of the unfolded protein response appeared to be involved in the development of hepatic steatosis in FL-N/35 transgenic mice fed the excess-iron diet.

Reactive oxygen species generation and endoplasmic reticulum stress

Superoxide has been reported to be selectively involved in ER stress-mediated apoptosis (28). It is also reported that anti-oxidants reduce ER stress and improve protein secretion (29). These results suggest that ROS production induces ER stress. We evaluated *in situ* ROS production in the liver by staining with dihydroethidium and assessed whether treatment with an anti-oxidant reduced hepatic steatosis through inhibition of the unfolded protein response. ROS production was significantly higher in FL-N/35

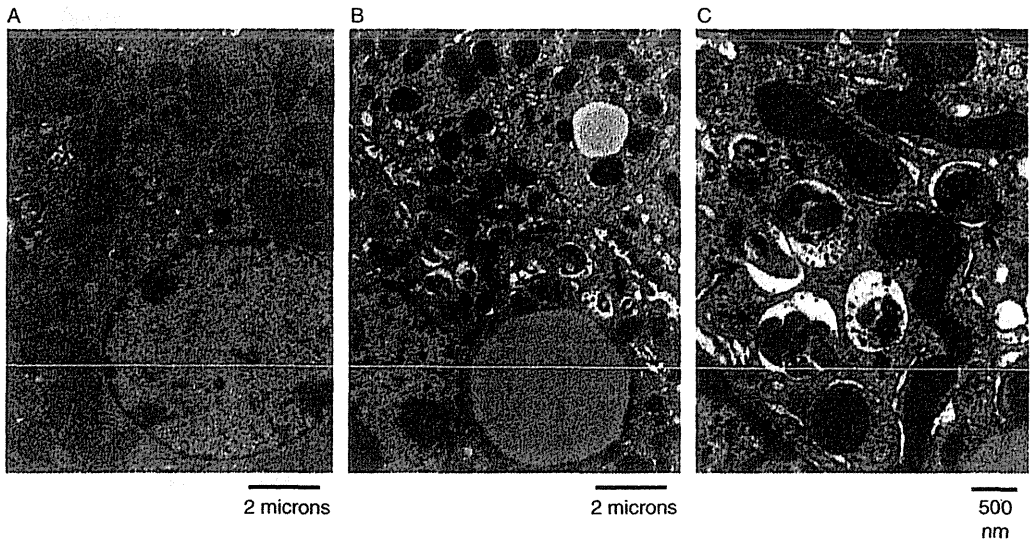

Fig. 4. Electron microscopy of the liver of an FL-N/35 transgenic mouse and a nontransgenic mouse, both of which were fed the excess-iron diet for 12 months. (A) Nontransgenic mouse, (B) full-length HCV-N open reading frame (FL-N/35) transgenic mouse and (C) Magnified picture of B. Autophagosomes (indicated by arrows) are abundantly found in the liver of the FL-N/35 transgenic mouse fed the excess-iron diet. Magnification scales are indicated below each picture.

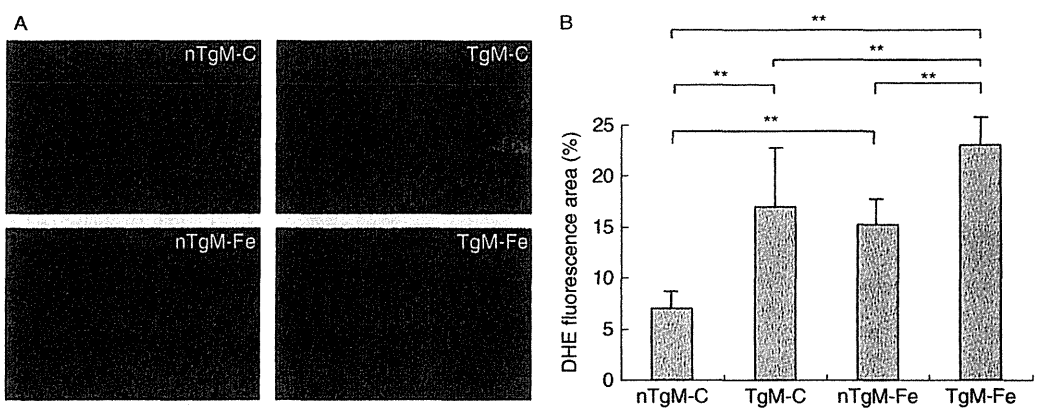

Fig. 5. Reactive oxygen species production in the liver. (A) Frozen liver sections of mice in each group were stained with dihydroethidium. (B) Fluorescence intensity was quantified by NIH image analysis software for three randomly selected areas of digital images for three mice in each group at 12 months after initiation of iron loading. $^{**}P < 0.01$. nTgM-C, TgM-C, nTgM-Fe, and TgM-Fe; see legend for Figure 1.

transgenic mice fed the excess-iron diet than in mice in the three other groups, even though abundant ROS production was found in all mice, except for nontransgenic mice fed the control diet (Fig. 5A and B). ROS production was significantly higher in transgenic mice than in nontransgenic mice irrespective of iron overloading. Iron overloading also significantly increased ROS production irrespective of whether the mice were transgenic or nontransgenic (Fig. 5B). FL-N/35 transgenic mice fed the excess-iron diet had the highest level of ROS production.

A six-month treatment with an anti-oxidant, NAC, dramatically reduced hepatic steatosis in FL-N/35 transgenic mice fed the excess-iron diet (Fig. 6A), together

Fig. 6. Liver histology, and the ratio of liver weight to body weight, serum alanine aminotransferase (ALT) levels, reactive oxygen specie's production and expression of carnitine palmitoyl transferase I (CPT1), sterol-regulatory element-binding protein I (SREBP1), spliced X-box DNA-binding protein 1 (sXBP1), unspliced X-box DNA-binding protein 1 (uXBP1) and CCAAT/enhancer-binding protein homology protein (CHOP) in the liver of full-length HCV-N open reading frame (FL-N/35) transgenic mouse fed the excess-iron diet with/without *N*-acetyl cysteine (NAC) treatment. (A) NAC treatment drastically reduced hepatic steatosis in mice. (B) Frozen liver sections of mice in each group were stained with dihydroethidium. Fluorescence intensity was quantified with the method described in the legend for Figure 5 in three mice in each group. (C)

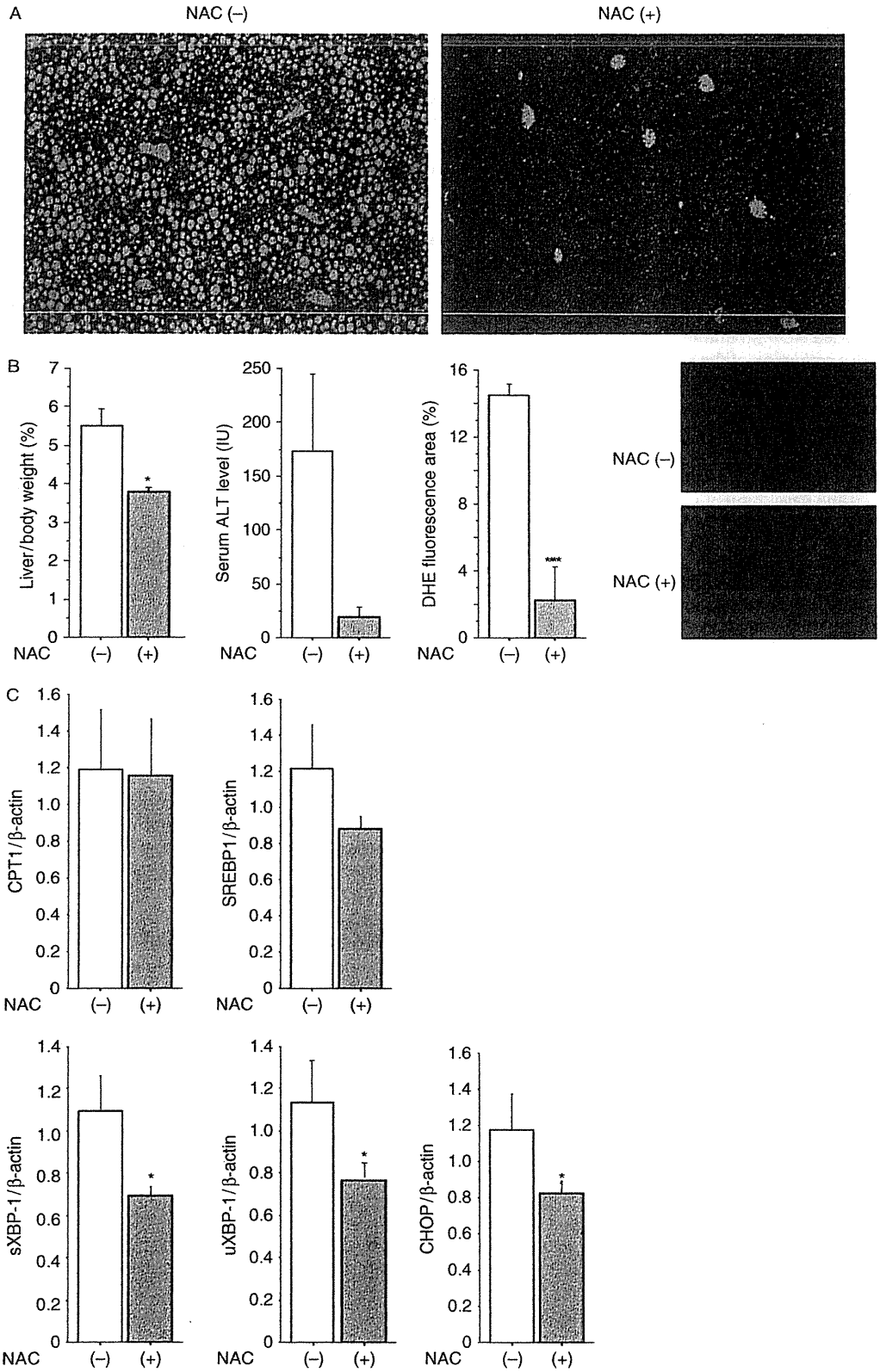

with a significant reduction in the ratio of liver weight to body weight and ROS production (Fig. 6B). The serum alanine aminotransferase level was also reduced by NAC, but this change was not statistically significant because of the large variance of the data. The expression of uXBP1, sXBP1 and CHOP was significantly reduced after treatment with NAC, suggesting an inhibitory effect of the anti-oxidant on the unfolded protein response (Fig. 6C). The expression of SREBP1 was also reduced by treatment with NAC, but this reduction was not statistically significant ($P = 0.08$). The expression of CPT1, which regulates oxidization of long-chain fatty acids in the mitochondria, did not change after NAC treatment. These results suggested that iron-induced ROS generation induced hepatic steatosis through the activation of the unfolded protein response. It also seemed that the increased lipogenesis through the activated unfolded protein response contributed more to the development of hepatic steatosis than the reduced β-oxidation activity in FL-N/35 transgenic mice fed the excess-iron diet, because the anti-oxidant almost completely inhibited the development of hepatic steatosis without affecting the expression of CPT1.

Discussion

The hepatic iron content of FL-N/35 transgenic mice fed the excess-iron diet was comparable to that of a large number of patients with chronic hepatitis C in extensive studies (15, 16). The positive correlation between the iron level and the triglyceride concentration in the liver was consistent with our previous observation that even modest iron supplementation enhanced hepatic steatosis in FL-N/35 transgenic mice (9), suggesting a potential role of iron in the development of HCV-related steatosis. Although previous studies revealed a direct contribution of HCV core protein to the development of hepatic steatosis (5–7), how iron overload, which is one of pathological features in chronic hepatitis C, affects hepatic steatosis remains unknown. The decreased expression of CPT I suggested reduced β-oxidation activity, because this transmembrane enzyme of the mitochondrial outer membrane has been shown to be the rate-limiting step in the β-oxidation of long-chain fatty acids (30). This result was consistent with our previous observation that the degradation activity of fatty acids *in vivo* was reduced in iron-overloaded transgenic mice. The decreased expression of CPT I may be related to the association of HCV core protein with the mitochondrial outer membrane (31). However, the decreased expression of CPT I seemed to reflect the rather increased synthesis of fatty acids because CPT I is negatively regulated by malonyl-CoA, an intermediate product in fatty acid synthesis, at the transcriptional level (30). In fact, the expression of FAS was significantly increased in FL-N/35 transgenic mice fed the excess-iron diet, which was presumably driven by upregulation of a transcription factor, SREBP1. We could not differentiate SREBP1c from SREBP1a at the protein level because of the lack of an adequate antibody; nevertheless, the expression of SREBP1 was assumed to mainly reflect that of SREBP1c, because the SREBP1c transcript extremely predominates over the SREBP1a transcript in the mouse liver (32).

The regulation of SREBP activation occurs at two levels: transcriptional and post-transcriptional (17). Upregulation of SREBP1c promoter activity has been reported in HCV core gene-transgenic mice (6), but we did not find a significant difference in SREBP1 expression between transgenic and nontransgenic mice without iron overloading. This contradiction may have arisen from a difference in the transgenic mice used in the two studies. In addition, a recent report found no significant difference in the hepatic expression of SREBP1c mRNA between subjects with HCV infection and those with a histologically normal liver (33). HCV has been demonstrated to induce proteolytic cleavage of SREBP1 and 2 in HCV replicon cells (34). As described previously, modest iron supplementation restored a major phenotype of FL-N/35 transgenic mice marked by hepatic steatosis and liver tumour development (9). Thus, the present animal model was useful for understanding the critical role of iron overloading in the development of HCV-related hepatic steatosis. We therefore focused on the post-transcriptional regulation of SREBP1 by iron in the presence of HCV proteins. Upon ER stress, the SREBP–SCAP complex dissociates from the ER retention protein and subsequently translocates to the Golgi apparatus, where SREBP is cleaved and activated (18, 19). FL-N/35 transgenic mice fed the excess-iron diet showed the activated unfolded protein response, assessed by the increased expression of uXBP-1, sXBP-1, p-eIF2α and CHOP, suggesting that the unfolded protein response was activated by iron overloading in the presence of HCV proteins. On the other hand, it is demonstrated that the trans-activating activity of XBP-1 is suppressed, but ATF6 functions properly in HCV replicon cells (35), which is in part contradictory to the present results. Methodological differences (*in vivo* or *in vitro*, iron overload or not, etc.) in two studies may account for this contradiction. Thus, the role of the unfolded protein response in HCV infection alone is still a matter of debate.

To confirm activation of the unfolded protein response in FL-N/35 transgenic mice fed the excess-iron diet, we wanted to assess not only the activation of ER-resident sensors but also the morphological change induced by the unfolded protein response. Autophagy has been shown to play important roles in cell survival after ER stress (25–27). A double-membrane structure, which is called the autophagosome or the autophagic vacuole, is formed *de novo* to sequester cytoplasm. Then the vacuole membrane fuses with the lysosomal membrane to deliver the contents into the autolysosome, where they are degraded and the resulting macromolecules are recycled. Some studies demonstrated a critical role of IRE1 in inducing autophagy under ER stress (25, 36), whereas another study reported the involvement of the PERK-eIF2α signalling pathway, not IRE1, in autophagy induction by ER stress (37). Thus, it is still controversial as to

which transducer is utilized for ER stress-induced autophagy in mammalian cells. The abundant presence of autophagosomes was consistent with the activation of both ER-resident sensors, IRE1 and PERK, in the liver in FL-N/35 transgenic mice fed the excess-iron diet. Although there is no direct link between induction of autophagy and hepatic steatosis in FL-N/35 transgenic mice fed the excess-iron diet, induction of autophagy seemed to support the ER stress-related hepatic steatosis because autophagy is one of the morphological changes under ER stress (25–27).

Iron overload is potentially one of multiple sources of ROS production, as represented in the iron-catalysed Fenton reaction (38). FL-N/35 transgenic mice fed the excess-iron diet had a significantly higher level of ROS production than mice in the three other groups, suggesting a cooperative role of HCV proteins and iron in inducing oxidative stress. ROS have been demonstrated to be involved upstream of the unfolded protein response (28). Anti-oxidants have also been shown to reduce the unfolded protein response and improve protein secretion (29). The present findings that the expression of uXBP1, sXBP1 and CHOP, but not CPT1, was significantly reduced with NAC treatment were consistent with these previous observations, suggesting that iron-induced ROS activated the unfolded protein response in the presence of HCV proteins. How then does ER stress activate SREBP1? There are several lines of evidence suggesting that one mechanism by which ER stress leads to activation of SREBPs is related to downregulation of insulin-induced genes. Downregulation of insulin-induced genes is associated with less retention of SREBPs in the ER, which leads to increased SREBP activation (39–41). As another mechanism, it has been shown that overexpression of glucose-regulated protein 78, one of the ER resident chaperone proteins, inhibits SREBP activation (42). Irrespective of how ER stress activates SREBP, the predominant role of SREBP1 in the ER stress-related hepatic steatosis in FL-N/35 transgenic mice fed the excess-iron diet was similar to that observed in a murine intragastric ethanol-feeding model (43). In conclusion, considering the complexity of the argument and the limited number of evaluated mechanisms, iron-induced ROS-activated unfolded protein response may be postulated as one of the possible mechanisms of HCV-related fat accumulation in the liver.

Acknowledgements

This study was supported by a grant from the Ministry of Education, Culture, Sports, Science and Technology (No. 20590782), and in part by the Ministry of Health, Labor and Welfare, Japan.

References

1. Scheuer PJ, Ashrafzadeh P, Sherlock S, Brown D, Dusheiko GM. The pathology of hepatitis C. *Hepatology* 1992; **15**: 567–71.
2. Farinati F, Cardin R, De Maria N, *et al.* Iron storage, lipid peroxidation and glutathione turnover in chronic anti-HCV positive hepatitis. *J Hepatol* 1995; **22**: 449–56.
3. Ohata K, Hamasaki K, Toriyama K, *et al.* Hepatic steatosis is a risk factor for hepatocellular carcinoma in patients with chronic hepatitis C virus infection. *Cancer* 2003; **97**: 3036–43.
4. Kato J, Kobune M, Nakamura T, *et al.* Normalization of elevated hepatic 8-hydroxy-2′-deoxyguanosine levels in chronic hepatitis C patients by phlebotomy and low iron diet. *Cancer Res* 2001; **61**: 8697–702.
5. Perlemuter G, Sabile A, Letteron P, *et al.* Hepatitis C virus core protein inhibits microsomal triglyceride transfer protein activity and very low density lipoprotein secretion: a model of viral-related steatosis. *FASEB J* 2002; **16**: 185–94.
6. Moriishi K, Mochizuki R, Moriya K, *et al.* Critical role of PA28γ in hepatitis C virus-associated steatogenesis and hepatocarcinogenesis. *Proc Natl Acad Sci USA* 2007; **104**: 1661–6.
7. Tanaka N, Moriya K, Kiyosawa K, *et al.* PPARα activation is essential for HCV core protein-induced hepatic steatosis and hepatocellular carcinoma in mice. *J Clin Invest* 2008; **118**: 683–94.
8. Nishina S, Hino K, Korenaga M, *et al.* Hepatitis C virus-induced reactive oxygen species raise hepatic iron level in mice by reducing hepcidin transcription. *Gastroenterology* 2008; **134**: 226–38.
9. Furutani T, Hino K, Okuda M, *et al.* Hepatic iron overload induces hepatocellular carcinoma in transgenic mice expressing the hepatitis C virus polyprotein. *Gastroenterology* 2006; **130**: 2087–98.
10. Beard MR, Abell G, Honda M, *et al.* An infectious molecular clone of a Japanese genotype 1b hepatitis C virus. *Hepatology* 1999; **30**: 316–24.
11. Lerat H, Honda M, Beard MR, *et al.* Steatosis and liver cancer in transgenic mice expressing the structural and nonstructural proteins of hepatitis C virus. *Gastroenterology* 2002; **122**: 352–65.
12. Bligh EG, Dyer WJ. A rapid method of total lipid extraction and purification. *Can J Biochem Physiol* 1959; **37**: 911–7.
13. Lowry OH, Rosebrough NJ, Farr AL, Randall RJ. Protein measurement with the Folin phenol reagent. *J Biol Chem* 1951; **193**: 265–75.
14. Harrison-Findik DD, Schafer D, Klein E, *et al.* Alcohol metabolism-mediated oxidative stress down-regulates hepcidin transcription and leads to increased duodenal iron transporter expression. *J Biol Chem* 2006; **281**: 22974–82.
15. Hofer H, Osterreicher C, Jessner W, *et al.* Hepatic iron concentration does not predict response to standard and pegylated-IFN/ribavirin therapy in patients with chronic hepatitis C. *J Hepatol* 2004; **40**: 1018–22.
16. Rulyak SJ, Eng SC, Patel K, *et al.* Relationships between hepatic iron content and virologic response in chronic hepatitis C patients treated with interferon and ribavirin. *Am J Gastroenterol* 2005; **100**: 332–7.
17. Horton JD, Goldstein JL, Brown MS. SREBPs: activators of the complete program of cholesterol and fatty acid synthesis in the liver. *J Clin Invest* 2002; **109**: 1125–31.

18. Brown MS, Goldstein JL. The SREBP pathway: regulation of cholesterol metabolism by proteolysis of a membrane-bound transcription factor. *Cell* 1997; **89**: 331–40.
19. Ron D, Oyadomari S. Lipid phase perturbations and the unfolded protein response. *Dev Cell* 2004; **7**: 287–8.
20. Ji C, Kaplowitz N. ER stress: can the liver cope? *J Hepatol* 2006; **45**: 321–33.
21. Calfon M, Zeng H, Urano F, *et al.* IRE1 couples endoplasmic reticulum load to secretory capacity by processing the XBP-1 mRNA. *Nature* 2002; **415**: 92–6.
22. Yoshida H, Matsui T, Yamamoto A, Okada T, Mori K. XBP1 mRNA is induced by ATF6 and spliced by IRE1 in response to ER stress to produce a highly active transcription factor. *Cell* 2001; **107**: 881–91.
23. Marciniak SJ, Ron D. Endoplasmic reticulum stress signaling in disease. *Physiol Rev* 2006; **86**: 1133–49.
24. Okada T, Yoshida H, Akazawa R, Negishi M, Mori K. Distinct roles of activating transcription factor 6 (ATF6) and double-stranded RNA-activated protein kinase-like endoplasmic reticulum kinase (PERK) in transcription during the mammalian unfolded protein response. *Biochem J* 2002; **366**: 585–94.
25. Ogata M, Hino S, Saito A, *et al.* Autophagy is activated for cell survival after endoplasmic reticulum stress. *Mol Cell Biol* 2006; **26**: 9220–31.
26. Yorimitsu T, Nair U, Yang Z, Klionsky DJ. Endoplasmic reticulum stress triggers autophagy. *J Biol Chem* 2006; **281**: 30299–304.
27. Yin XM, Ding WX, Gao W. Autophagy in the liver. *Hepatology* 2008; **47**: 1773–85.
28. Yokouchi M, Hiramatsu N, Hayakawa K, *et al.* Involvement of selective reactive oxygen species upstream of proapoptotic branches of unfolded protein response. *J Biol Chem* 2008; **283**: 4252–60.
29. Malhotra JD, Miao H, Zhang K, *et al.* Antioxidants reduce endoplasmic reticulum stress and improve protein secretion. *Proc Natl Acad Sci USA* 2008; **105**: 18525–30.
30. Kerner J, Hoppel C. Fatty acid import into mitochondria. *Biochim Biophys Acta* 2000; **1486**: 1–17.
31. Korenaga M, Wang T, Li Y, *et al.* Hepatitis C virus core protein inhibits mitochondrial electron transport and increases reactive oxygen species (ROS) production. *J Biol Chem* 2005; **280**: 37481–8.
32. Shimomura I, Shimano H, Horton JD, Goldstein JL, Brown MS. Differential expression of exons 1a and 1c in mRNAs for sterol regulatory element binding protein-1 in human and mouse organs and cultured cells. *J Clin Invest* 1997; **99**: 838–45.
33. McPherson S, Jonsson JR, Barrie HD, *et al.* Investigation of the role of SREBP-1c in the pathogenesis of HCV-related steatosis. *J Hepatol* 2008; **49**: 1046–54.
34. Waris G, Felmlee DJ, Negro F, Siddiqui A. Hepatitis C virus induces proteolytic cleavage of sterol regulatory element binding proteins and stimulates their phosphorylation via oxidative stress. *J Virol* 2007; **81**: 8122–30.
35. Tardif KD, Mori K, Kaufman RJ, Siddiqui A. Hepatitis C virus suppresses the IRE1-XBP1 pathway of the unfolded protein response. *J Biol Chem* 2004; **279**: 17158–64.
36. Yorimitsu T, Klionsky DJ. Endoplasmic reticulum stress: a new pathway to induce autophagy. *Autophagy* 2007; **3**: 160–2.
37. Kouroku Y, Fujita E, Tanida I, *et al.* ER stress (PERK/eIF2alpha phosphorylation) mediates the polyglutamine-induced LC3 conversion, an essential step for autophagy formation. *Cell Death Differ* 2007; **14**: 230–9.
38. Fenton HJH. Oxidation of tartaric acid in presence of iron. *J Chem Soc* 1894; **65**: 899–910.
39. Engelking LJ, Kuriyama H, Hammer RE, *et al.* Overexpression of Insig-1 in the livers of transgenic mice inhibits SREBP processing and reduces insulin-stimulated lipogenesis. *J Clin Invest* 2004; **113**: 1168–75.
40. Engelking LJ, Liang G, Hammer RE, *et al.* Schoenheimer effect explained – feedback regulation of cholesterol synthesis in mice mediated by Insig proteins. *J Clin Invest* 2005; **115**: 2489–98.
41. Flury I, Garza R, Shearer A, *et al.* INSIG: a broadly conserved transmembrane chaperone for sterol-sensing domain proteins. *EMBO J* 2005; **24**: 3917–26.
42. Werstuck GH, Lentz SR, Dayal S, *et al.* Homocysteine-induced endoplasmic reticulum stress causes dysregulation of the cholesterol and triglyceride biosynthetic pathways. *J Clin Invest* 2001; **107**: 1263–73.
43. Ji C, Chan C, Kaplowitz N. Predominant role of sterol response element binding proteins (SREBP) lipogenic pathways in hepatic steatosis in the murine intragastric ethanol feeding model. *J Hepatol* 2006; **45**: 717–24.

IMMUNOLOGY & MEDICAL MICROBIOLOGY

RESEARCH ARTICLE

Molecular typing of *Bartonella henselae* DNA extracted from human clinical specimens and cat isolates in Japan

Masashi Yanagihara[1,2], Hidehiro Tsuneoka[3], Shoko Hoshide[4], Erina Ishido[4], Akiko Umeda[1], Masato Tsukahara[5], Junzo Nojima[1], Kiyoshi Ichihara[3], Keisuke Hino[6], Itaru Hirai[2] & Yoshimasa Yamamoto[2]

[1]Department of Basic Laboratory Sciences, Yamaguchi University Graduate School of Medicine, Yamaguchi, Japan; [2]Department of Biomedical Informatics, Osaka University Graduate School of Medicine, Osaka, Japan; [3]Department of Clinical Laboratory Sciences, Yamaguchi University Graduate School of Medicine, Yamaguchi, Japan; [4]Faculty of Health Sciences, Yamaguchi University School of Medicine, Yamaguchi, Japan; [5]Yamaguchi University Graduate School of Medicine, Yamaguchi, Japan; and [6]Department of Hepatology and Pancreatology, Kawasaki Medical University, Okayama, Japan

Correspondence: Masashi Yanagihara, Department of Basic Laboratory Sciences, Yamaguchi University Graduate School of Medicine, 1-1-1 Minami-kogushi, Ube, Yamaguchi 755-8505, Japan.
Tel./fax: +81 836 22 2838;
e-mail: m-yanagi@yamaguchi-u.ac.jp

Received 31 January 2010; revised 10 May 2010; accepted 25 May 2010.

DOI:10.1111/j.1574-695X.2010.00711.x

Editor: Ewa Sadowy

Keywords
Bartonella henselae; cat scratch disease; multilocus sequence typing (MLST); 16S–23S tRNA-Ala/tRNA-Ile intergenic spacer.

Abstract

Bartonella henselae is the causative agent of cat scratch disease (CSD). To clarify the population structure and relationship between human and cat strains of *B. henselae*, 55 specimens isolated in Japan, including 24 *B. henselae* DNA-positive clinical samples from CSD patients and 31 *B. henselae* isolates from domestic cats, were characterized by multilocus sequence typing (MLST) and the 16S–23S tRNA-Ala/tRNA-Ile intergenic spacer (S1) sequence, which were used previously for strain typing of *B. henselae*. Three different sequence types (STs) were identified by MLST, one of which was novel. Fifty-two strains (94.5%), including all strains detected in CSD patients, were assigned to ST-1. Eight S1 genotypes were observed, three of which were novel. The 52 ST-1 strains were classified into seven S1 genotypes, two of which were predominant in both human and cat strains. In addition, 5.5% of the strains (3/55) contained two different intergenic spacer S1 copies. These results indicate that the predominant *B. henselae* MLST ST-1 in Japan is a significantly genetically diverse population on the basis of the sequence diversity of intergenic spacer S1, and that highly prevalent S1 genotypes among cats are often involved in human infections.

Introduction

Bartonella henselae is the causative agent of cat scratch disease (CSD). Cats represent the major reservoir for *B. henselae*. Infected cats are usually asymptomatic and develop relapsing bacteremia for long periods (Kordick *et al.*, 1995). Human infection usually occurs through scratches or bites by infected cats and presents as CSD, typically with localized lymphadenopathy. Occasionally, the infection may have an atypical presentation due to blood-borne spread, such as bacteremia, endocarditis, encephalopathy, neuroretinitis, or systemic CSD with hepatic and splenic granuloma (Anderson & Neuman, 1997; Murakami *et al.*, 2002; Tsuneoka & Tsukahara, 2006). Disease symptoms depend on the immune status of the host; in immunocompromised hosts, the bacteria are often present in blood and involved in angioproliferative disorders such as bacillary angiomatosis and peliosis hepatis (Welch *et al.*, 1992).

Isolation of *B. henselae* from patients is extremely difficult (La Scola & Raoult, 1999). The diagnosis of CSD relies on clinical manifestations, history of contact with cats, serology, or the detection of bacterial DNA in tissue specimens by PCR (Regnery *et al.*, 1992; Anderson *et al.*, 1994; Murakami *et al.*, 2002; Woestyn *et al.*, 2004; Tsuneoka & Tsukahara, 2006). *Bartonella henselae* strains are divided into two 16S rRNA (*rrs*) genotypes (16S type I/Houston-1 and 16S type II/Marseille), which correspond to two distinct human serotypes (Drancourt *et al.*, 1996; La Scola *et al.*, 2002). Although both genotypes are present worldwide, 16S type II appears to be dominant in the European cat population, whereas 16S type I is more common in Asia, including Japan (Maruyama *et al.*, 2000; Boulouis *et al.*, 2005).

Multilocus sequence typing (MLST) is a nucleotide sequencing-based genotyping method in which variations in approximately 450–500-bp internal fragments of

housekeeping genes (generally seven) are indexed (Maiden, 2000). MLST analysis of 182 feline and human *B. henselae* isolates from Europe, North America, and Australia revealed that sequence type (ST)-1 was most significantly associated with human infection, but that the geographical distribution of STs was not homogenous (Arvand *et al.*, 2007). However, the use of highly conserved housekeeping genes in MLST often fails to detect variability in closely related strains. Compared with housekeeping genes, intergenic spacers are highly variable, thus generating a clearer population structure (Li *et al.*, 2009). In the multispacer typing (MST) scheme for *B. henselae*, the 16S–23S tRNA-Ala/tRNA-Ile intergenic spacer (S1) is the most variable spacer, containing a 15-bp variable number tandem repeat (VNTR) (Li *et al.*, 2006). PCR-based genotyping methods can be applied directly to clinical specimens (Rodrick *et al.*, 2004; Li *et al.*, 2007). However, no data are available regarding the predominant strains causing CSD in Japan.

In this study, we examined 55 human and feline *B. henselae* specimens by MLST and S1 sequence to uncover the genotypic distribution and relationship between human and cat strains of *B. henselae* in Japan. Furthermore, we analyzed the structural diversity of ST-1 using the intergenic spacer S1 sequence to generate a clear population structure.

Materials and methods

Clinical specimens

Twenty-four human clinical specimens consisted of five lymph node specimens and 16 pus specimens from patients with typical CSD, one blood specimen from a patient with bacteremia, one liver specimen from a patient with hepatic granuloma, and one spleen specimen from a patient with splenic granuloma. The specimens were obtained from various regions of western Japan, including Yamaguchi prefecture, from 1997 to 2008.

Bacterial strains

The 31 *B. henselae* isolates were derived from 290 blood samples collected from domestic cats in western Japan, mainly Yamaguchi prefecture, from 2003 to 2004 (Tsuneoka *et al.*, 2004). Primary isolates of *B. henselae* from cat blood samples were grown on chocolate agar plates with 5% defibrinated sheep blood at 35 °C in 5% carbon dioxide (CO_2) for 2 weeks. The strains were stored at − 80 °C until use. Subcultures were performed on chocolate agar plates with 5% defibrinated sheep blood at 35 °C in 5% CO_2 for 5 days. A single colony of each isolate was passaged once on agar before the extraction of bacterial DNA.

DNA extraction

Total genomic DNA was extracted using the QIAamp DNA Mini Kit (Qiagen, Hilden, Germany) according to the manufacturer's instructions.

Identification of *B. henselae*

Bartonella henselae was detected with PCR targeting 414 bp of the *htrA* gene and 172 bp of the *Bartonella* species-specific 16S–23S rRNA internal transcribed spacer region, and confirmed by partial sequencing of the 16S rRNA gene using broad-host-range primer 16SF together with 16SR, as described previously (Anderson *et al.*, 1994; Bergmans *et al.*, 1996; Jensen *et al.*, 2000). No bacterial species other than *B. henselae* was detected in any sample.

PCR amplification and sequencing

For MLST, eight genes (*rrs*, *batR*, *gltA*, *ftsZ*, *groEL*, *nlpD*, *ribC*, and *rpoB*) were amplified and sequenced directly using MLST primers for *B. henselae* as described previously (Iredell *et al.*, 2003). The intergenic spacer S1 was amplified and sequenced directly using S1 forward primer and S1 reverse primer as described previously (Li *et al.*, 2007). When direct sequencing of spacer S1 was unsuccessful because of an atypical number of VNTRs, locus-specific PCR was performed using S1 forward primer with one of two locus-specific primers: BH12700-R (5′-ACGCCAATGT GTTATCCACTT-3′) or BH13810-R (5′-GAAACTTGTCGA TGATCAGGC-3′). The PCR mixture contained 1 × Phusion HF Buffer (Finnzymes, Espoo, Finland), 0.4 U Phusion DNA polymerase (Finnzymes), 200 μM dNTP, 500 nM of each primer, 4–100 ng DNA template, and sterile-distilled water, in a final volume of 20 μL. The reaction conditions were as follows: denaturation at 98 °C for 30 s; 35–50 cycles at 98 °C for 10 s, 56–62 °C for 30 s, and 72 °C for 30–120 s; and a final extension step at 72 °C for 10 min. PCR products were purified using the High Pure PCR Product Purification Kit (Roche Diagnostics GmbH, Mannheim, Germany) and then sequenced directly using the BigDye Terminator v3.1 Cycle Sequencing Kit (Applied Biosystems, Foster City, CA) on both strands with a 3130 Genetic Analyzer (Applied Biosystems).

Sequencing analysis and phylogenetic analysis

The nucleotide sequences were analyzed with DNA SEQUENCING ANALYSIS software version 5.1 (Applied Biosystems). Alleles, STs, and S1 genotypes were assigned in accordance with published data (Iredell *et al.*, 2003; Li *et al.*, 2006, 2007; Arvand *et al.*, 2007). The novel allele and S1 sequence were carefully confirmed on multiple occasions, and the sequences were deposited in the DNA Data Bank of Japan (DDBJ). New S1 genotypes were deposited in the MST-Rick

database (http://ifr48.timone.univ-mrs.fr/MST_BHenselae/mst). A neighbor-joining tree was reconstructed from the concatenated MLST allele sequences of 14 previously reported STs (Iredell *et al.*, 2003; Arvand *et al.*, 2007) and the novel ST-15 using Kimura 2-parameter distance measures as implemented in MEGA4 (Tamura *et al.*, 2007).

Nucleotide sequence accession numbers

Newly encountered sequences have been submitted to DDBJ under the following accession numbers: AB525232, *rpoB* allele 5 (YC-073); AB525233, S1 genotype 11 (YC-053); and AB534165, S1 genotype 12 (YC-012 and YC-013).

Results and discussion

MLST analysis detected three STs in 55 human and cat *B. henselae* strains. Intriguingly, 94.5% (52/55) of *B. henselae* strains including all 24 human clinical specimens were assigned to ST-1, and only three cat isolates were assigned to other STs (Table 1). In isolate YC-073, a new allele was found in *rpoB*, which consisted of a single nucleotide variation (G instead of A) at position 711 784 of the *B. henselae* Houston-1 chromosome (accession no. BX897699). The ST containing this allele was designated as ST-15. Phylogenetic tree analysis revealed that ST-15 belongs to Group 1 and is closely related to ST-1 (Fig. 1). In the MLST analysis, ST-1 was common among cat isolates, and human clinical specimens were assigned to ST-1 at a much higher frequency (100%) than that observed in previous studies (Iredell *et al.*, 2003; Lindroos *et al.*, 2006; Arvand *et al.*, 2007). However, the clonal population of ST-1 in Japan is quite different from that reported in other regions.

To generate a clearer population structure, we analyzed the 55 strains using the highly variable intergenic spacer S1. We identified eight different S1 genotypes, three of which were novel (Table 2). S1 genotype 11 containing a sixfold repetition of the 15-bp sequence was found in YC-053. S1 genotype 12 with a single nucleotide deletion at position 1 412 654 of the *B. henselae* Houston-1 (accession no. BX89 7699) was found in YC-012 and YC-013. The third novel S1 genotype was found in three cat isolates YC-015, YC-024, and YC-073, which contained atypical numbers of VNTRs in the two spacer S1 regions (Fig. 2). The complete genome sequence of *B. henselae* Houston-1 (accession no. BX897699) was shown to contain two identical copies of intergenic spacer S1. Locus-specific PCR, followed by direct sequencing revealed that these isolates were assigned to S1 genotype 7+4 (Fig. 2 and Table 3).

Compared with MLST, the intergenic spacer S1 was able to generate a clearer population structure of the strains under investigation. The 52 ST-1 strains were classified into seven distinct S1 genotypes. Our results indicate that ST-1 has a high genetic diversity on the basis of the sequence diversity of intergenic spacer S1. MLST could not clearly differentiate between strains because the eight selected

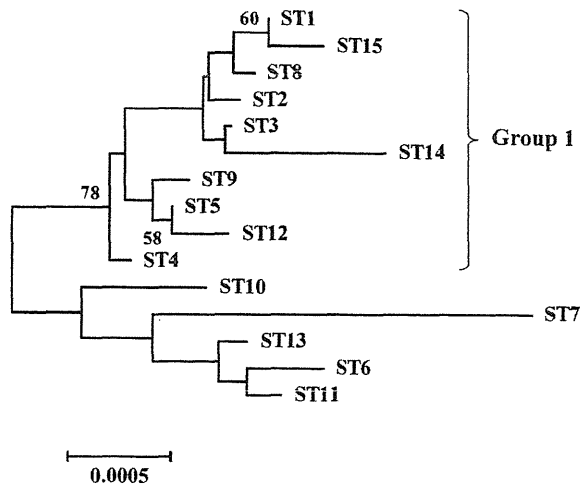

Fig. 1. Neighbor-joining tree of concatenated MLST allele sequences of 15 *Bartonella henselae* STs. Concatenated MLST allele sequences representing each ST were obtained for 14 previously reported STs and the new ST-15, and a neighbor-joining tree was generated by performing bootstrap analyses (1000 replicates) using MEGA4. Only node values > 50% are indicated in the figure.

Table 1. Multilocus sequence typing of 31 *Bartonella henselae* isolates from domestic cats

	Allele number								No. of
ST	*rrs*	*batR*	*gltA*	*ftsZ*	*groEL*	*nlpD*	*ribC*	*rpoB*	isolates (*n*)
1	1	1	1	1	1	1	1	1	28
6	2	3	2	2	2	1	1	2	2*
15	1	1	1	1	1	1	1	5	1†

**Bartonella henselae* isolates YC-012 and YC-013.
†*Bartonella henselae* isolate YC-073.

Table 2. Distribution of intergenic spacer S1 genotypes among 55 human and cat *Bartonella henselae* strains

	No. of strains (*n*)	
S1 genotype	Human	Cat
3	1	0
4	12	14
5	9	10
7	1	1
8	1	0
11	0	1
12	0	2
7+4*	0	3

*S1 genotype 7+4 indicates that the strain had two different copies of intergenic spacer S1 in its genome.

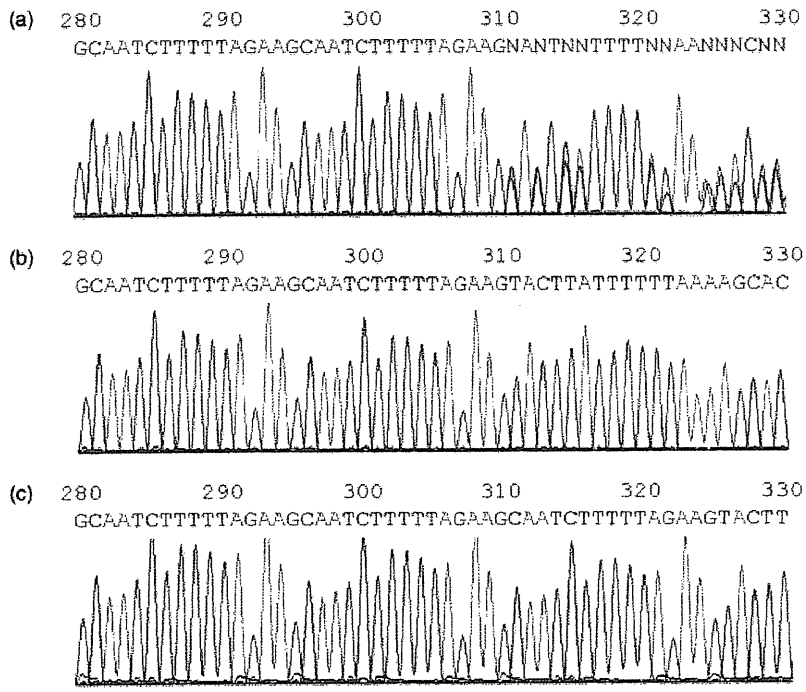

Fig. 2. Representative results of direct sequencing of the 16S–23S tRNA-Ala/tRNA-Ile intergenic spacer (S1) in *Bartonella henselae* strain YC-015. These sequences show the 15-bp VNTR (CAATCTTTTTAGAAG) detected with the S1 forward primer. (a) The sequence, obtained from PCR using the S1 forward and reverse primers, shows the abrupt onset of ambiguous bases suggestive of overlapping sequences. (b) The sequence corresponding to the 1 412 349–1 412 683 position of BX897699, obtained from PCR using the S1 forward and BH12700-R primers, shows a double repetition of the 15-bp VNTR and belongs to S1 genotype 7. (c) The sequence corresponding to the 1 582 358–1 582 692 position of BX897699, obtained from PCR using the S1 forward and BH13810-R primers, shows a triple repetition of the 15-bp VNTR and belongs to S1 genotype 4. The same results were obtained from *B. henselae* strains YC-024 and YC-073.

Table 3. Profiles of S1 genotype at two different positions in the YC-015, YC-024, and YC-073 strains

	Spacer position on the genome*	
	1 412 349–1 412 683	1 582 358–1 582 692
S1 genotype	7	4
No. of 15-bp repeat	2	3

**Bartonella henselae* Houston-1 (accession no. BX897699).

housekeeping genes were highly conserved and showed less sequence variability.

According to the intergenic spacer S1 sequence, two major S1 genotypes, 4 and 5, were identified in both human and cat strains (Table 2). In a previous MST study of *B. henselae* specimens isolated from patients in France, only S1 genotypes 3 (53.3%) and 5 (45.3%) were observed (Li *et al.*, 2007). S1 genotype 3 was not a predominant genotype in our study, and S1 genotype 4 was not detected in France. This discrepancy may be explained by similar regional differences observed in the distribution of S1 genotypes 3 and 4 among cats in France (Li *et al.*, 2006) and Japan, respectively. These data suggest that prevalent S1 genotypes among cats are often involved in human infections. Further studies are necessary to elucidate the association of the S1 genotype with pathogenicity.

In conclusion, we have demonstrated that the predominant *B. henselae* MLST in Japan, ST-1, is a significantly genetically diverse population on the basis of the sequence diversity of intergenic spacer S1, and that highly prevalent S1 genotypes among cats are often involved in human infections. These results may aid our understanding of the population structure and the relationship between human and cat strains of *B. henselae*.

Acknowledgements

This work was supported by Grant-in-Aid for Young Scientists (B) No. 21790538 from the Ministry of Education, Culture, Sports, Science and Technology of Japan.

References

Anderson B, Sims K, Regnery R, Robinson L, Schmidt MJ, Goral S, Hager C & Edwards K (1994) Detection of *Rochalimaea henselae* DNA in specimens from cat scratch disease patients by PCR. *J Clin Microbiol* **32**: 942–948.

Anderson BE & Neuman MA (1997) *Bartonella* spp. as emerging human pathogens. *Clin Microbiol Rev* **10**: 203–219.

Arvand M, Feil EJ, Giladi M, Boulouis HJ & Viezens J (2007) Multi-locus sequence typing of *Bartonella henselae* isolates from three continents reveals hypervirulent and feline-associated clones. *PLoS One* **2**: e1346.

Bergmans AM, Schellekens JF, van Embden JD & Schouls LM (1996) Predominance of two *Bartonella henselae* variants

among cat-scratch disease patients in the Netherlands. *J Clin Microbiol* **34**: 254–260.

Boulouis HJ, Chang CC, Henn JB, Kasten RW & Chomel BB (2005) Factors associated with the rapid emergence of zoonotic *Bartonella* infections. *Vet Res* **36**: 383–410.

Drancourt M, Birtles R, Chaumentin G, Vandenesch F, Etienne J & Raoult D (1996) New serotype of *Bartonella henselae* in endocarditis and cat-scratch disease. *Lancet* **347**: 441–443.

Iredell J, Blanckenberg D, Arvand M, Grauling S, Feil EJ & Birtles RJ (2003) Characterization of the natural population of *Bartonella henselae* by multilocus sequence typing. *J Clin Microbiol* **41**: 5071–5079.

Jensen WA, Fall MZ, Rooney J, Kordick DL & Breitschwerdt EB (2000) Rapid identification and differentiation of *Bartonella* species using a single-step PCR assay. *J Clin Microbiol* **38**: 1717–1722.

Kordick DL, Wilson KH, Sexton DJ, Hadfield TL, Berkhoff HA & Breitschwerdt EB (1995) Prolonged *Bartonella* bacteremia in cats associated with cat-scratch disease patients. *J Clin Microbiol* **33**: 3245–3251.

La Scola B & Raoult D (1999) Culture of *Bartonella quintana* and *Bartonella henselae* from human samples: a 5-year experience (1993 to 1998). *J Clin Microbiol* **37**: 1899–1905.

La Scola B, Liang Z, Zeaiter Z, Houpikian P, Grimont PA & Raoult D (2002) Genotypic characteristics of two serotypes of *Bartonella henselae*. *J Clin Microbiol* **40**: 2002–2008.

Li W, Chomel BB, Maruyama S, Guptil L, Sander A, Raoult D & Fournier PE (2006) Multispacer typing to study the genotypic distribution of *Bartonella henselae* populations. *J Clin Microbiol* **44**: 2499–2506.

Li W, Raoult D & Fournier PE (2007) Genetic diversity of *Bartonella henselae* in human infection detected with multispacer typing. *Emerg Infect Dis* **13**: 1178–1183.

Li W, Raoult D & Fournier PE (2009) Bacterial strain typing in the genomic era. *FEMS Microbiol Rev* **33**: 892–916.

Lindroos H, Vinnere O, Mira A, Repsilber D, Naslund K & Andersson SG (2006) Genome rearrangements, deletions, and amplifications in the natural population of *Bartonella henselae*. *J Bacteriol* **188**: 7426–7439.

Maiden MC (2000) High-throughput sequencing in the population analysis of bacterial pathogens of humans. *Int J Med Microbiol* **290**: 183–190.

Maruyama S, Nakamura Y, Kabeya H, Tanaka S, Sakai T & Katsube Y (2000) Prevalence of *Bartonella henselae, Bartonella clarridgeiae* and the 16S rRNA gene types of *Bartonella henselae* among pet cats in Japan. *J Vet Med Sci* **62**: 273–279.

Murakami K, Tsukahara M, Tsuneoka H, Iino H, Ishida C, Tsujino K, Umeda A, Furuya T, Kawauchi S & Sasaki K (2002) Cat scratch disease: analysis of 130 seropositive cases. *J Infect Chemother* **8**: 349–352.

Regnery RL, Olson JG, Perkins BA & Bibb W (1992) Serological response to "*Rochalimaea henselae*" antigen in suspected cat-scratch disease. *Lancet* **339**: 1443–1445.

Rodrick D, Dillon B, Dexter M, Nicholson I, Marcel S, Dickeson D & Iredell J (2004) Culture-negative endocarditis due to Houston complex *Bartonella henselae* acquired in Noumea, New Caledonia. *J Clin Microbiol* **42**: 1846–1848.

Tamura K, Dudley J, Nei M & Kumar S (2007) MEGA4: Molecular Evolutionary Genetics Analysis (MEGA) software version 4.0. *Mol Biol Evol* **24**: 1596–1599.

Tsuneoka H & Tsukahara M (2006) Analysis of data in 30 patients with cat scratch disease without lymphadenopathy. *J Infect Chemother* **12**: 224–226.

Tsuneoka H, Ishida C, Umeda A, Inokuma H & Tsukahara M (2004) Evaluation of isolation media for the detection of *Bartonella henselae* – isolation of *Bartonella henselae* from domestic cats. *Kansenshogaku Zasshi* **78**: 574–579.

Welch DF, Pickett DA, Slater LN, Steigerwalt AG & Brenner DJ (1992) *Rochalimaea henselae* sp. nov., a cause of septicemia, bacillary angiomatosis, and parenchymal bacillary peliosis. *J Clin Microbiol* **30**: 275–280.

Woestyn S, Olive N, Bigaignon G, Avesani V & Delmee M (2004) Study of genotypes and *virB4* secretion gene of *Bartonella henselae* strains from patients with clinically defined cat scratch disease. *J Clin Microbiol* **42**: 1420–1427.

腫瘍内科，6(5)：419-424，2010　　6：419

特集　肝がんの治療戦略―最近の動向

肝細胞がんの発癌予防の現状と展望*

池田健次**

Key Words：hepatocellular carcinoma, interferon, hepatitis C, hepatitis B, nucleoside analogue

はじめに

肝癌のほとんどは，肝炎ウイルスやアルコールなど何らかの原因による慢性肝疾患に発生する．このうち，わが国ではB型肝炎・C型肝炎ウイルスが肝癌の原因の約90％を占めている．本稿では，これらウイルス性肝炎に対する「原因療法」である抗ウイルス療法や「対症療法」である抗炎症療法による肝癌発癌抑制効果について述べる．

C型慢性肝炎に対するインターフェロン療法の肝発癌抑制効果

当院で腹腔鏡肝生検により確定診断したC型慢性肝炎について，インターフェロン治療の有無およびその治療効果により発癌率がどの程度の影響を受けるかをretrospectiveコホートにより検討した[1)2)]．

1．対　象

対象は1970年より2000年までの間に診断したC型慢性肝炎2,166例．全例HBs抗原陰性で，診断時の初期血清にてHCV抗体陽性，HCVRNA陽性が確認されている．男性は1,421例，女性745例，年齢の中央値は50歳(14～78歳)であった．インターフェロン治療を行った例は1,654例(76.4％)，行わなかったのは512例で，無治療例はインターフェロンが導入される1987年以前の症例が多かった．

2．方　法

インターフェロンの治療効果は，SVR(インターフェロン終了24週間後HCVRNA陰性化)，BR(インターフェロン終了後6か月以上ALT正常化)，NR(上記以外の効果)に分け，発癌率の検討を行った．

経過観察からの脱落例は223例(10.3％)で，インターフェロン群164例(9.9％)，無治療群59例(11.5％)であった．全体の症例の観察期間は0.1年から33.6年，中央値は10.7年であった．発癌率はKaplan-Meier法で行い，治療有無別・治療効果別の発癌率はログランクテストで行った．発癌率に寄与する要因は，Cox比例ハザードモデルで検討した．

3．成　績

(1)インターフェロンの治療効果

1,654例に行ったインターフェロンの治療効果は，SVR 606例(36.6％)，BR 266例(16.1％)，NR 782例(47.3％)であった．

(2)肝癌発癌率

中央値10.7年の間に，199例(9.2％)の肝癌発癌がみられた．このうち，96例はインターフェロン治療例(96/1,654, 9.2％)，103例は無治療例(103/512, 20.1％)であった．

粗発癌率は，インターフェロン治療群・無治

* Perspective of prevention of hepatocellular carcinogenesis.

** Kenji IKEDA, M.D.: 国家公務員共済組合連合会虎の門病院肝臓センター〔〒105-8470 東京都港区虎ノ門2-2-2〕; Department of Hepatology, Toranomon Hospital, Tokyo 105-8470, JAPAN

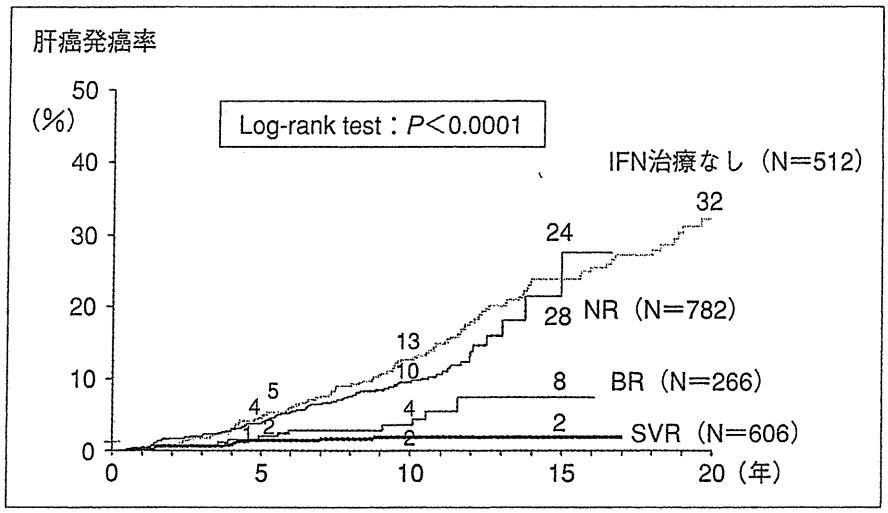

図1　インターフェロン(IFN)治療効果別にみたC型慢性肝炎からの肝癌発癌率

療群でそれぞれ，5年2.6%，4.6%，10年5.8%，12.7%，15年13.9%，23.9%で，インターフェロン治療群での発癌率は有意に低かった($P<0.0001$，ログランクテスト)．

(3)インターフェロン治療効果別にみた肝癌発癌率(図1)

インターフェロン施行例から発癌した96例のうち，SVRから発癌したのは11例(1.8%)，BRからは10例(3.8%)，NR例からは75例(9.6%)が発癌した．SVR・BR・NR別にみた粗発癌率は，5年1.4%，2.0%，3.8%，10年1.9%，3.6%，9.6%，15年1.9%，7.5%，27.6%であった．SVR群・BR群での発癌率はNR群より有意に低率であった($P<0.0001$)．

(4) C型慢性肝炎からの発癌に寄与する要因

多変量解析では，肝線維化程度(F3でのハザード比8.68, $P<0.001$)，GGTP(50以上のハザード比2.64, $P<0.001$)，性別(男性のハザード比2.38, $P<0.001$)，インターフェロン治療の有無(インターフェロン治療のハザード比0.42, $P<0.001$)，低血小板数(10万未満でのハザード比2.22, $P<0.001$)，年齢(50歳以上のハザード比1.90, $P=0.002$)の6要因が肝癌発癌に有意に関連する要因であった．インターフェロン治療により，発癌ハザードは0.42に低下すると計算された．

(5)インターフェロン治療効果別にみた肝癌発癌リスク

肝癌発癌に寄与する要因は，肝線維化程度(F3でのハザード比9.90, $P<0.001$)，性別(男性のハザード比3.44, $P<0.001$)，GGTP(50以上のハザード比2.68, $P=0.008$)，年齢(50歳以上のハザード比2.56, $P=0.001$)，AFP(20ng/ml以上のハザード比2.34, $P=0.003$)，低血小板数(10万未満でのハザード比2.09, $P=0.013$)があげられ，これらの共変量で補正した場合，無治療に対するSVRのハザード比は0.10($P<0.001$)，BRでは0.12($P<0.001$)，NRでは0.57($P=0.46$)であった．SVR・BR達成は有意に発癌率低下をもたらした．

4．インターフェロンの発癌抑制効果の位置づけ

2,166例と多数例のC型慢性肝炎のretrospective cohort studyからわかったことは，①インターフェロン治療を行うと(社会全体の)C型慢性肝炎からの発癌率が有意に低下すること，②インターフェロン治療でSVR・BRが得られると，無治療に比べて1/10近くまでの発癌率低下が得られることである．ことに，ウイルス排除に至らなくても，トランスアミナーゼがインターフェロン後一定期間以上の正常値を維持するだけで発癌リスクが著明に低下することの意義は大きい．

C型慢性肝炎に対するグリチルリチン製剤投与の肝発癌抑制効果

インターフェロン治療でSVR・BRが得られなかった症例に対して，グリチルリチン製剤(強力ネオミノファーゲン・シー™，以下SNMCと略)を使用し，その発癌抑制効果を1,249例のretrospective cohort studyで検討した[3)4)]．

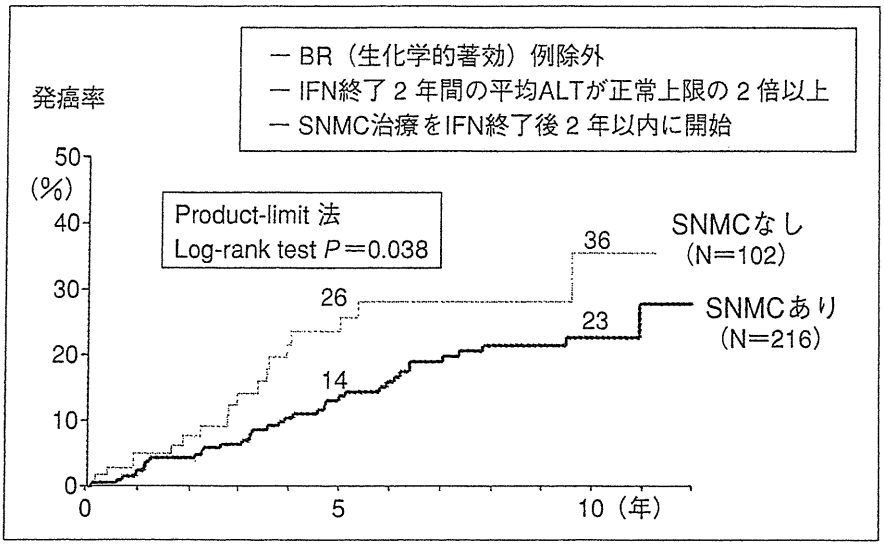

図2　強力ネオミノファーゲン・シー™(SNMC)投与別にみたインターフェロン(IFN)無効C型慢性肝炎からの粗肝癌発癌率

1．対象・方法

1987年から2002年の間に当院でインターフェロン治療を行い，投与終了後6か月の時点でHCV-RNAが陽性であった1,249例を対象とした．症例の年齢は中央値53歳，男性778例・女性471例，慢性肝炎1,142例，肝硬変107例であった．SNMC治療を行ったのは453例，行わなかった例は796例で，前者ではインターフェロン無効判定時，年齢が有意に高く，AST・ALTが高く，また肝硬変の頻度が有意に高かった．

2．成　　績

(1)SNMC治療群・非治療群での粗発癌率

治療群・非治療群での5年発癌率はそれぞれ11.6%，5.0%，10年発癌率は19.9%，10.6%で，SNMC治療群で有意に高率であった(P=0.0001)．

(2)インターフェロン終了1年の平均ALT値別にみた発癌率

平均ALTを以下の6群に分けて発癌率を比較した：正常，正常値の1.5倍以内，1.5から2倍，2から3倍，3から4倍，4倍以上．それぞれの10年発癌率は，6.6%，7.2%，19.6%，15.1%，21.0%，39.3%で，平均ALT値と発癌率とは明らかな相関がみられた．

(3)インターフェロン後活動性の症例での発癌率

インターフェロン後にSNMCが使用された症例は，年齢・肝線維化・トランスアミナーゼなどすべてが発癌リスクの高い側に偏っており，インターフェロン使用例と同様のトランスアミナーゼ値の症例について，無治療例と比較して発癌率の検討を行った．

インターフェロン後に不完全著効と判定された例を除外し，かつ平均ALT値が正常値の2倍以上であった418例(SNMC群289例，非治療群129例)について発癌率を比較した．SNMCはインターフェロン治療後にトランスアミナーゼが上昇し2年以内に治療を開始した症例のみに限って検討した．このような背景の症例で，SNMC群・非治療群の肝癌発癌率を比較すると，5年発癌率は13.3%，26.0%，10年発癌率は21.5%，35.5%で，SNMC群で有意に発癌率が低かった(P=0.021)(図2)．

(4)インターフェロン無効後の発癌に寄与する独立要因

インターフェロン無効の判定後SNMC治療を開始するまでの期間を時間依存性変数として，発癌率に寄与する要因を多変量解析で検討した．肝線維化の程度(F1に比しF2～F3のハザード比2.94，F4のハザード比9.21，P<0.001)・性別(男性のハザード比2.80，P=0.006)・SNMCの有無(有のハザード比0.49，P=0.014)が独立して肝癌発癌に有意に関連した要因であった．

3．グリチルリチン投与の意義

インターフェロンが無効であったC型慢性肝疾患症例にグリチルリチン製剤(SNMC)の長期投与を行い肝癌発癌率に及ぼす影響を1,249例の

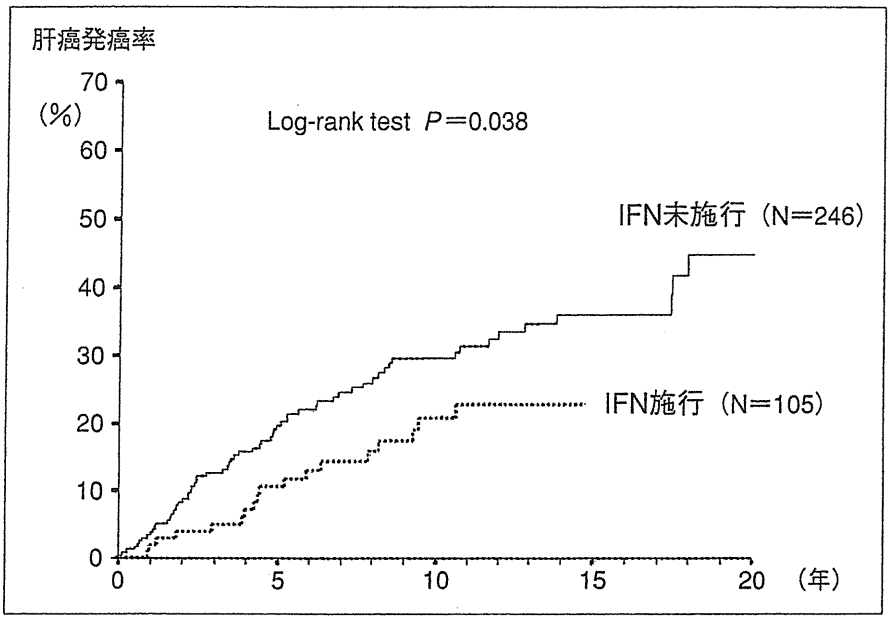

図3　インターフェロン(IFN)の投与有無別にみたB型肝硬変からの肝癌発癌率

多数例について検討した．インターフェロン無効例中，トランスアミナーゼが正常の2倍以上の高値症例でかつインターフェロン終了後2年以内に治療開始した症例についてみると，SNMC投与群では肝癌発癌率は有意に低くなった(P=0.021)．また，時間依存性比例ハザードモデルで発癌に寄与する要因を多変量解析で検討しても，肝線維化などの共変量で補正してもグリチルリチン製剤使用により発癌ハザードが0.49と有意に低下し，壊死炎症を抑制する肝庇護療法でも発癌抑制に役立つことが明らかとなった．

B型肝硬変に対するインターフェロンの肝発癌抑制効果

B型慢性肝炎は年率0.5～1％の発癌率で相対的に発癌率が低いため，ここでは抗ウイルス剤による発癌抑制効果を検討するため，B型肝硬変を対象とした．すなわち，B型肝硬変をコホートとして，インターフェロン(IFN)の発癌抑制効果についてretrospectiveな検討を行った[5]．

1．対象・方法

対象は，1974年より1995年までの間に腹腔鏡肝生検で確定診断されたHBs抗原陽性・HCV抗体陰性のB型肝硬変313例で，IFN治療を行った94例(30.0％)とIFN治療を行わなかった219例との肝癌発癌率を比較した．

IFN治療を行った群と行わなかった群での背景因子を比較すると，IFN治療群では年齢の中央値は41歳で未治療群より3歳若年で，男性例の比率がやや高かった．また，治療群ではe抗原陽性率が65.6％で未治療群の46.0％より有意に高く，トランスアミナーゼ値も高値の傾向であった．

IFN治療は1日600万単位のαまたはβ-IFNの投与を基本とし，週2回の間歇投与を6か月もしくはそれ以上の期間行った．治療を行った94例での投与期間の中央値は10か月で，2例は5年間を超えて長期投与を行った．94例中2例では4万/mm³以下の血小板減少に至り，IFNの投与量減量を必要とした．そのほか，精神症状や骨髄抑制などの副作用により投与を中止した症例はなかった．

経過観察よりの脱落例は24例(7.7％)のみであり，この症例も含めた経過観察期間の中央値は7.0年(最短0.1年，最長22.3年)であった．

全例HBVDNAを1年1回経時的に測定し，病態との関連を検討した．検体はすべて－80℃保存の凍結血清を用いて行った．

統計学的方法としては，ノンパラメトリック手法による検定，発癌率はKaplan-Meier法，発癌率の差はログランクテストで行い，P<0.05を有意水準とした．

2．成　　績

(1)粗肝癌発癌率の比較(図3)

観察期間の中央値7.0年の間に，IFN治療群・

未治療群からはそれぞれ10例(10.6%)，51例(21.3%)の発癌例がみられた．IFN治療群・未治療群での3年累積発癌率はそれぞれ4.5%，13.3%，5年発癌率はそれぞれ，7.0%，19.6%，10年はそれぞれ17.0%，30.8%で，IFN治療群では有意に発癌率が低かった(log-rank test, $P=0.012$)．

(2)発癌に寄与する独立要因

多変量解析の結果，B型肝硬変からの肝癌発癌に影響する因子は，①積算飲酒量($P=0.028$)，②AFP値($P=0.011$)，③ICGR15分値($P=0.029$)，④IFN使用(ハザード比0.39, $P=0.031$)の4要因が独立要因であり，IFNの使用により発癌率が低下することが示された．

すなわち，IFNを使用しない状態では，B型肝硬変からの発癌率を高める要因は，積算飲酒量が500kg以上であること(これより少ない例と比べて3.27倍のハザード比)，AFP値が20ng/m*l*以上(20ng/m*l*未満に比し3.02倍のハザード比)，ICGR15分値が30%以上の例(30%未満の例に比し2.20倍のハザード比)であった．Retrospectiveな研究であるので，これら発癌率に有意に影響する3要因で治療群・非治療群の背景因子を同等となるように多変量解析を行うと，IFN治療により発癌ハザードが0.39に低下し($P=0.031$)，明らかにIFNがB型肝硬変からの発癌を抑制することが判明した．

(3) B型肝硬変に対するIFN治療の現状と今後

IFNの短期療法は高率にHBVの再燃をきたすため，ここではIFNを6か月以上の長期間歇的に使用する方法で行うことが重要である．これはretrospectiveな研究であるが，単変量および多変量解析にて，IFN長期療法が発癌率を有意に低下させることが判明した．

3．考　察

IFNが発癌抑制効果を示すひとつの理由として考えられるのは，微小な早期肝癌に対する直接的な抗癌作用であり，もうひとつはIFNの持つ抗ウイルス活性である．肝細胞の破壊・再生に基づく肝細胞回転の亢進状態を，IFNの抗ウイルス効果が間接的に発癌抑制的に作用する可能性である．そのほか，IFNの発癌抑制効果の理由としてさらに，肝細胞回転を介さない直接的な抗ウイルス作用，抗発癌作用も推定される．

いずれにせよ，臨床的なB型肝硬変からの発癌抑制効果の成績を踏まえて，より基礎的なB型肝炎・肝硬変からの発癌メカニズムの解明が必要であり，その上でIFNの詳細な発癌抑制効果が研究される必要があると考えられる．

B型慢性肝炎に対するラミブジンの発癌抑制効果

核酸アナログ製剤のうち，長期の治療実績のあるラミブジン投与成績について，その発癌抑制効果を検討した．

対象は，当科でラミブジンを使用したB型慢性肝疾患3,674例のうち，肝細胞癌を発生していない慢性肝炎・肝硬変3,539例を対象としてretrospective cohort studyを行った．ラミブジン投与は706例，非投与は2,833例であった．

累積粗肝細胞癌発生率を投与群・非投与群で比較すると，3年・5年・7年・10年肝癌発生率は，投与例で2.2%，3.1%，4.0%，4.0%であったが，非投与例では2.3%，4.4%，6.2%，9.5%で，投与群で粗発癌率は低い傾向であった($P=0.14$)(図4)．比例ハザードモデルで肝癌発癌に寄与する独立要因は，性別(男性のハザード7.25, $P=0.001$)，肝線維化(F2, 3のハザード2.25, F4のハザード4.66, $P<0.001$)，初診年齢(35歳以上のハザード3.93, $P=0.005$)，初診時e抗原(陽性例のハザード2.00, $P=0.005$)で，これにラミブジン治療(なしのハザード1.68, $P=0.084$)が続いた．

当院で行ったretrospective studyでは，多変量解析でラミブジン投与例での発癌抑制傾向が示された．Liawら[6]は，651例の線維化進行B型慢性肝疾患例に対して無作為化比較試験を行い，ラミブジン投与により病変進行(非代償期移行，肝細胞癌発生，特発性細菌性腹膜炎発生，食道胃静脈瘤出血，肝疾患関連死亡)までの期間が延長するかの検討を行っている．このエンドポイントに達した人数はラミブジン群で7.8%，無治療群で17.7%であった(ハザード比0.45, $P=0.001$)．エンドポイントの内訳のうち，肝癌発症率はラミブジン群3.9%，無治療群7.4%で，治療群で発癌抑制がみられた(ハザード比0.49, $P=0.047$)．わが国からもretrospective cohort studyではあるものの，犬山研究会参加施設からの多

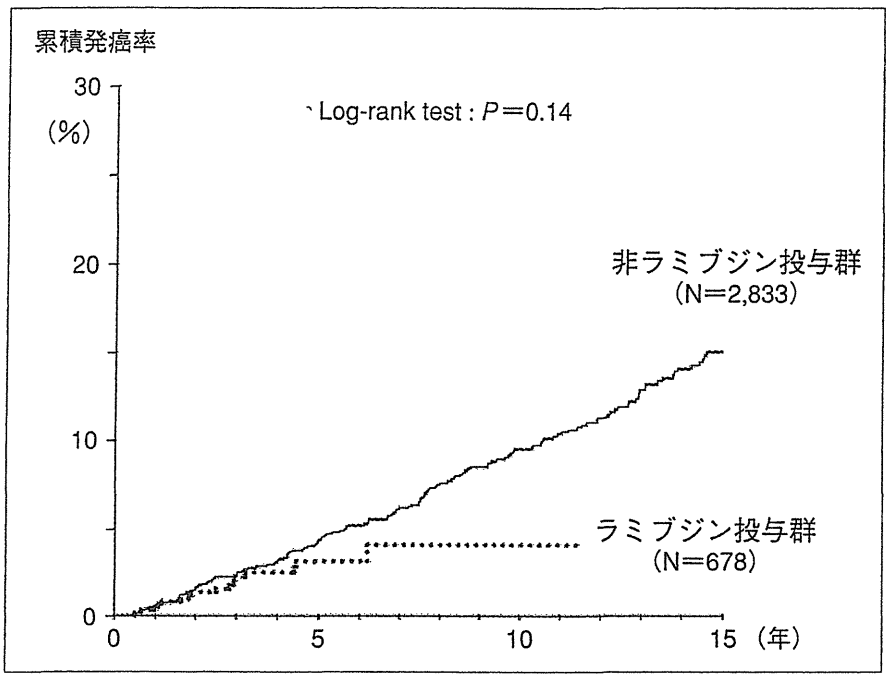

図4　ラミブジン投与別にみたB型慢性肝疾患からの粗肝癌発癌率

数例の解析[7]で，ラミブジンによる肝癌発癌抑制のデータが示された．症例は30施設から2,795例集積され，ラミブジン投与657例，非投与2,138例が比較されている．年齢・性別・肝線維化など7項目を合致させた各群377例のcohort的研究で肝癌発癌数をみると，ラミブジン群では4例(1.1%)発癌し，年率発癌率は0.4%であったのに対し，非ラミブジン群では50例(13.3%)に発癌がみられ，その年率発癌率は2.5%であった．

B型慢性肝疾患に対するインターフェロンによる発癌率抑制効果に関しては，これまで一致した成績が出ていないが，エンテカビルによる治療効果に関しても今後早期にデータが集積されることが期待されている．

文　献

1) Ikeda K, Saitoh S, Arase Y, et al. Effect of interferon therapy on hepatocellular carcinogenesis in patients with chronic hepatitis type C : A long-term observation study of 1,643 patients using statistical bias correction with proportional hazard analysis. Hepatology 1999 ; 29 : 1124-30.

2) Ikeda K, Arase Y, Saitoh S, et al. Anticarcinogenic impact of interferon on patients with chronic hepatitis C : a large-scale long-term study in a single center. Intervirology 2006 ; 49 : 82-90.

3) Ikeda K, Arase Y, Kobayashi M, et al. A long-term glycyrrhizin injection therapy reduces hepatocellular carcinogenesis rate in patients with interferon-resistant active chronic hepatitis C : a cohort study of 1249 patients. Dig Dis Sci 2006 ; 51 : 603-9.

4) Ikeda K. Glycyrrhizin injection therapy prevents hepatocellular carcinogenesis in patients with interferon-resistant active chronic hepatitis C. Hepatol Res 2007 ; 37 : S287-93.

5) Ikeda K, Saitoh S, Suzuki Y, et al. Interferon decreases hepatocellular carcinogenesis in patients with cirrhosis caused by hepatitis B virus : a pilot study. Cancer 1998 ; 82 : 827-35.

6) Liaw YF, Sung JJ, Chow WC, et al.; Cirrhosis Asian Lamivudine Multicentre Study Group. Lamivudine for patients with chronic hepatitis B and advanced liver disease. N Engl J Med 2004 ; 351 : 1521-31.

7) Matsumoto A, Tanaka E, Rokuhara A, et al.; Inuyama Hepatitis Study Group. Efficacy of Lamivudine for preventing hepatocellular carcinoma in chronic hepatitis B : A multicenter retrospective study of 2795 patients. Hepatol Res 2005 ; 32 : 173-84.

臨牀消化器内科 2010 Vol.25 No.4
©日本メディカルセンター

特集 肝癌診療のアルゴリズム 2010

3 肝癌発生の危険因子と高危険群の設定 (1) B型慢性肝炎・肝硬変に発生する肝癌

池田 健次*

Key words: 肝発癌，B型肝炎ウイルス，慢性肝炎，肝硬変，高危険群

要 旨

抗ウイルス薬を投与しないB型慢性肝炎症例からの発癌率は5年2.9%，10年7.2%，15年9.9%で，B型肝硬変からの発癌率は5年19.7%，10年29.8%，15年36.3%であった．これらは同病期のC型慢性肝疾患からの発癌率の約半分の率であった．発癌率を高める要因は，進行肝病変，多飲酒歴，高齢，男性，低い血小板数，e抗原陽性，ICGR15高値などが挙げられるほか，B型肝硬変では，血中DNA量の経時的経過が発癌リスクと強い関係にあった．非進行B型肝疾患からの肝癌発癌は，すべての症例を肝癌高危険群として十分に囲い込むことは困難であり，危険性が相対的に低いこれらの症例をいかにサーベイランスしていくかはまだ解決されていない．

はじめに

肝細胞癌(肝癌)のほとんどは，肝炎ウイルスやアルコールなどなんらかの原因による慢性肝疾患に発生する．このうち，わが国ではB型肝炎・C型肝炎ウイルスが肝癌の原因の約85%を占めており，B型肝炎ウイルスが原因の肝癌は約15%を占めるとされている．

本稿では，わが国でのB型慢性肝炎・肝硬変からの発癌率を概観し，肝癌発癌に寄与する要因を慢性肝炎・肝硬変別に検討する．B型肝炎での発癌過程はC型肝炎とは異なり，HBVウイルス量に関連する事実や，HBs抗原消失後など，特殊な肝癌発癌状況についても記す．

*虎の門病院肝臓センター
(〒105-8470 東京都港区虎の門2-2-2)

Ⅰ．自然経過におけるB型慢性肝炎からの発癌率

この項のポイント

- B型慢性肝炎からの年率発癌率は0.5～1%で，線維化進行とともに発癌率は上昇する．

1. B型慢性肝炎からの肝癌発癌率

1976年から1998年までの間に当科で腹腔鏡肝生検により確定診断したB型慢性肝炎について，818例について検討した．全例初期血清でHBs抗原陽性・第Ⅱ世代HCV抗体陰性が測定されており，診断時に肝癌が合併していないことが確認されているが，このうち，これまでの経過観察期間にステロイド・インターフェロン・ラミブジンをまったく使用していない297例について発癌率の算出を行った．観察期間の中央値は8.6年(範囲：0.1～24年)であった．発癌率の計算はKaplan-Meier法，発癌率間の有意差検定はlog-rank testを使用した[1]．B型慢性肝炎297例からの累積肝癌発癌率は，5年

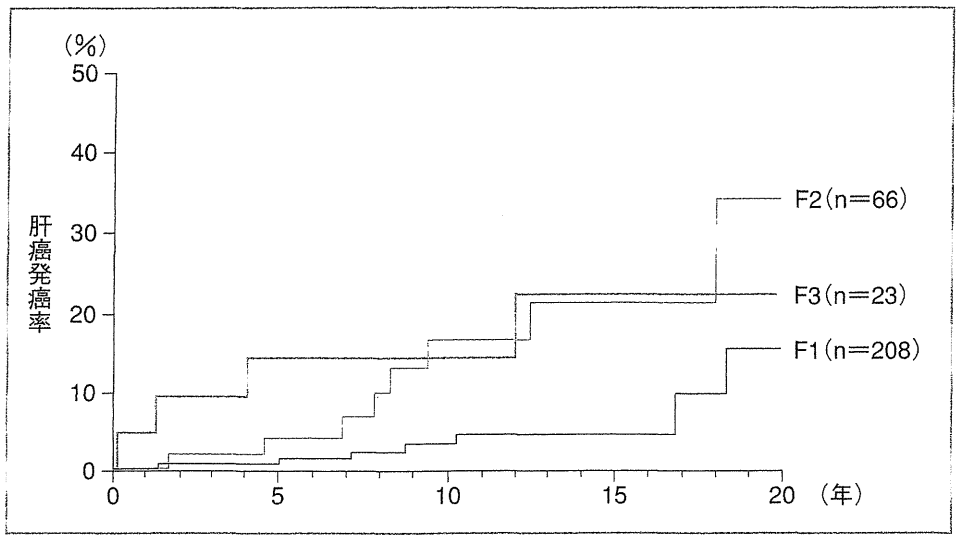

図1　新犬山分類別に見たB型慢性肝炎からの発癌率

2.9%，10年7.2%，15年9.9%，20年20.3%であった．これを新犬山分類による慢性肝炎進行度別に発癌率を検討すると，5年発癌率はF1(208例)，F2(66例)，F3(23例)でそれぞれ，0.5%，3.8%，14.0%，10年発癌率はそれぞれ3.0%，16.0%，14.0%，15年発癌率は4.2%，20.7%，21.8%，20年発癌率が14.9%，33.9%，21.8%であった(**図1**)．3群間には発癌率の有意差が認められた($P=0.0061$)が，C型慢性肝炎ではF1，F2，F3がこの順に発癌率が高くなっていくが，B型慢性肝炎ではやや異なり，F2とF3のステージで発癌率曲線に交叉が見られる現象が認められた．

2．B型慢性肝炎からの発癌に寄与する要因

無治療B型慢性肝炎297例について，肝癌発癌率を高める要因をCox比例ハザードモデルで検討した．多変量解析を行うと，①肝炎病期($P=0.0042$)，②多飲酒歴($P=0.027$)の2要因が独立要因として挙げられ，有意水準($P<0.05$)には達しないが，これに，③慢性肝炎診断時e抗原陽性($P=0.078$)が続いた．すなわち，F1病期に対しF2/F3病期では発癌ハザード比が4.14倍であり，慢性肝炎診断時までに多飲酒歴(総飲酒量が500 kg以上)の患者はそれ以外の患者に比し2.97のハザード比を示した．また，e抗原陽性例は陰性例に比して2.42の発癌ハザード比を示した．飲酒歴は年齢・性別要因と密接であるが，B型慢性肝炎からの発癌に対しては，肝炎病期のほかにウイルスの状態も関与していることが示唆される．

Ⅱ．自然経過におけるB型肝硬変からの発癌率

- B型肝硬変からの年率発癌率は約3%で，高齢，男性，血小板低値，e抗原陽性などが危険因子である．

1．B型肝硬変からの肝癌発癌率

1974年から1999年までの間に腹腔鏡肝生検で診断されたB型肝硬変245例について，肝癌発癌率をprospectiveに検討した．慢性肝炎の検討同様，全例初期血清でHBs抗原陽性・第Ⅱ世代HCV抗体陰性が測定されており，診断時に肝癌が合併していないことが確認されている．自然経過での肝癌発癌率の検討なので，すべての症例で，これまでの経過観察期間にステロイド・インターフェロン・ラミブジンをまっ

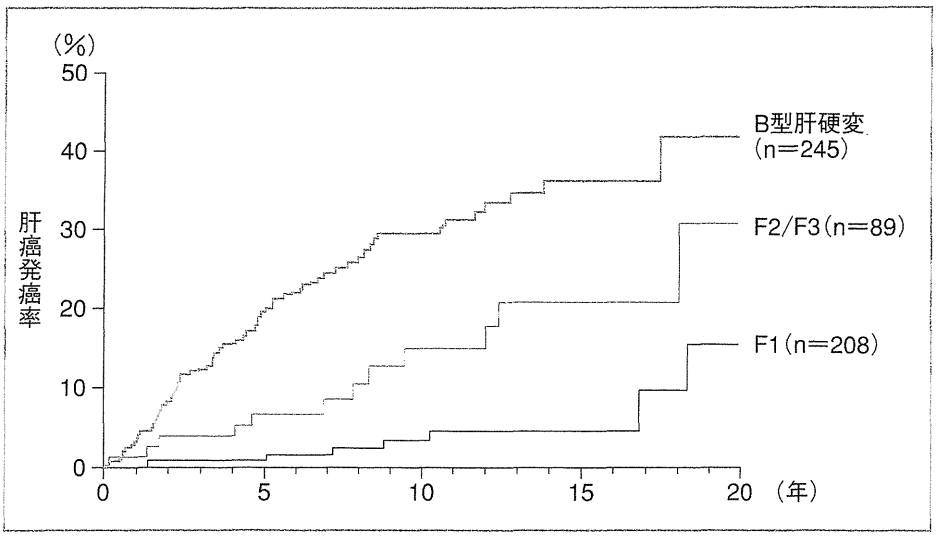

図2　B型慢性肝炎とB型肝硬変からの発癌率

たく使用していない．観察期間の中央値は6.9年(範囲：0.1～24年)であった[2]．

B型肝硬変245例からの累積肝癌発癌率は，5年19.7%，10年29.8%，15年36.3%，20年42.1%であった．これを新犬山分類別にみたB型慢性肝炎からの発癌率と比較すると(**図2**)，B型慢性肝炎より明らかに発癌率が高いことがわかる．図ではF2/F3を一つの発癌率曲線に示してあるが，B型肝硬変ではこのいずれよりも明らかに高い発癌率曲線を示し，F1，F2/F3，F4(肝硬変)となるに従って，発癌率が高くなっていくことが示された．

2．B型肝硬変からの発癌に寄与する要因

無治療B型肝硬変245例について，肝癌発癌率を高める要因をCox比例ハザードモデルで検討した．多変量解析を行うと，①年齢($P=0.0001$)，②性別($P=0.029$)，③血小板数($P=0.0079$)，④e抗原($P=0.019$)，の4要因が独立要因として挙げられ，有意水準($P<0.05$)には達しないが，これに，⑤ICG15分値($P=0.052$)が続いた．すなわち，45歳以上の肝硬変症例ではこれ未満の症例の4.33倍であり，男性では女性に対し発癌ハザードが4.63倍であった．さらに，血小板数が10万/mm^{3}未満の例はこれ以上の例に比し2.44倍の発癌ハザードを示し，e抗原陽性例は陰性例の2.19倍のハザード比を示した．

Ⅲ．B型肝硬変よりの発癌に及ぼすHBV DNA量の影響

この項のポイント

- B型肝硬変に進行した病態では，ALTよりHBV DNA値の経時的経過が発癌率に関係が強い．

B型肝硬変からの発癌に影響する要因が何であるかを検討するために，B型肝硬変症例について，長期経過観察しトランスアミナーゼ(ALT)・HBV DNAを経時的に測定し，肝癌発生がどのような臨床経過の後に発生するかを検討した[3]．

対象は当院で肝生検し確定診断されたB型肝硬変217症例の連続症例のうち，インターフェロンなどの抗ウイルス療法を行っていない160例とした．この160例で1年以上の観察例で全期間にわたる保存血清のある146例のうち最終的に肝癌発癌をみた例は48例(発癌までの平均観察期間7.2年)，観察終了時に未発癌であった例は98例(観察終了までの平均観察期間